Elucidating the Structural and Minimal Protective Epitope of the Serogroup X Meningococcal Capsular Polysaccharide

Gian Pietro Pietri, Marta Tontini, Barbara Brogioni, Davide Oldrini, Stefania Robakiewicz, Pedro Henriques, Ilaria Calloni, Vera Abramova, Laura Santini, Suzana Malić, et al.

Elucidating structural and minimal protective epitope of serogroup X meningococcal capsular polysaccharide

Gian P. Pietri[1], Marta Tontini[2], Barbara Brogioni[2], Davide Oldrini[2], Stefania Robakiewicz[3], Pedro Henriques[3, 2], Ilaria Calloni[4], Vera Abramova[1], Laura Santini[2], **Suzana Malić**[1], Karmela **Miklić**[2], **Berislav Lisnić**[1], Sara Bertuzzi[4], Luca Unione[4], Evita Balducci[2], Jérôme D. Ruyck[3], Maria Rosaria Romano[2], JESUS JIMENEZ-BARBERO[4], Julie Bouckaert[3], Stipan Jonjic[1], Tihana Lenac Roviš[1], Roberto Adamo[2*]

[1]University of Rijeka, Croatia, [2]GlaxoSmithKline (Italy), Italy, [3]Université de Lille, France, [4]CIC bioGUNE, Spain

Submitted to Journal:
Frontiers in Molecular Biosciences

Specialty Section:
Structural Biology

Article type:
Original Research Article

Manuscript ID:
745360

Received on:
21 Jul 2021

Journal website link:
www.frontiersin.org

Conflict of interest statement

The authors declare a potential conflict of interest and state it below

MT, BB, DO, PH, MRR and RA are employees of GSK group of companies. MRR and RA are inventors of patents related to this topic.

Author contribution statement

GP, JB, JJB, TLR, SJ and RA conceived the work; GP, MT, BB, DO, SR, PH, IC, VI, SM, KM, BL, SB, LU, EB, JR, MMR executed the work; GP, JB, TLR and RA wrote the manuscript; all contributed to the manuscript.

Keywords

structural glycobiology, glycoconhugates, Vaccines, Neisseria meningitidis, capsular polysaccharide

Abstract

Word count: 226

Despite the considerable progress towards the eradication of meningococcal disease with the introduction of glycoconjugate vaccines, previously unremarkable serogroup X has emerged in recent years, recording several outbreaks through the African continent. Different serogroup X polysaccharide-based vaccines have been tested in pre-clinical trials, establishing the principles for further improvement. To elucidate the antigenic determinants of the MenX capsular polysaccharide, we generated a monoclonal antibody, and its bactericidal nature was confirmed using the rabbit serum bactericidal assay. The antibody was tested by inhibition enzyme-linked immunosorbent assay and surface plasmon resonance against a set of oligosaccharide fragments of different lengths. The epitope was shown to be contained within 5 to 6 repeating units. The molecular interactions between the protective monoclonal antibody and the MenX capsular polysaccharide fragment were further detailed at atomic level by saturation transfer difference NMR spectroscopy. The NMR results were used for validation of the in-silico docking analysis between the x-ray crystal structure of the antibody (Fab fragment) and the modelled hexamer oligosaccharide. The antibody recognizes the MenX fragment by binding all 6 repeating units of the oligosaccharide via hydrogen bonding, salt bridges and hydrophobic interactions. In vivo studies demonstrated that conjugates containing 5-6 repeating units can produce high functional antibody levels. These results provide an insight on the molecular basis of MenX vaccine-induced protection and highlights the requirements for the epitope based vaccines design.

Contribution to the field

Identification of glycan epitopes is key for vaccine design. Meningococcal serogroup X has emerged in recent years as cause of outbreaks, particularly in the African continent. Different serogroup X polysaccharide-based vaccines have been tested in pre-clinical trials, establishing the principles for further improvement, however no information on structural and immunogenic epitope is known for this polysaccharide. Here we generated a functional mAb against MenX capsular polysaccharide, and we characterized the interactions with polysaccharide fragments by inhibition enzyme-linked immunosorbent assay and surface plasmon resonance. The epitope was shown to be contained within 5 to 6 repeating units. The molecular interactions between the protective monoclonal antibody and the MenX capsular polysaccharide fragment were further detailed at atomic level by saturation transfer difference NMR spectroscopy. The NMR results were used for validation of the in-silico docking analysis between the x-ray crystal structure of the antibody (Fab fragment) and the modelled hexamer oligosaccharide. The antibody recognizes the MenX fragment by binding all 6 repeating units of the oligosaccharide via hydrogen bonding, salt bridges and hydrophobic interactions. In vivo studies demonstrated that conjugates containing 5-6 repeating units can produce high functional antibody levels. These results highlight the potential of structural glycobiology to guide vaccines design.

Funding statement

This work was sponsored by GlaxoSmithKline Biologicals and has received funding from the European Union's Horizon 2020 Research and Innovation Programme under the Marie Skłodowska-Curie Grant Agreement 675671 and from SJ ("Strengthening the capacity of CerVirVac for research in virus immunology and vaccinology", grant no. KK.01.1.1.01.0006, awarded to the Scientific Centre of Excellence for Virus Immunology and Vaccines and co-financed by the European Regional Development Fund).

Ethics statements

Studies involving animal subjects

Generated Statement: The animal study was reviewed and approved by Italian Ministry of Health (Approval number n. 804/2015-PR)..

Studies involving human subjects

Generated Statement: No human studies are presented in this manuscript.

Inclusion of identifiable human data

Generated Statement: No potentially identifiable human images or data is presented in this study.

Data availability statement

Generated Statement: The datasets presented in this study can be found in online repositories. The names of the repository/repositories and accession number(s) can be found in the article/supplementary material.

Elucidating structural and minimal protective epitope of serogroup X meningococcal capsular polysaccharide

Gian Pietro Pietri[1], Marta Tontini[2], Barbara Brogioni[2], Davide Oldrini[2], Stefania Robakiewicz[3], Pedro Henriques[2], Ilaria Calloni[4], Vera Abramova[1], Laura Santini[b], Suzana Malić[1], Karmela Miklić[1], Berislav Lisnic[1], Sara Bertuzzi[4], Luca Unione[4], Evita Balducci[2], Jérôme de Ruyck[3], Maria Rosaria Romano[2], Jesus Jimenez-Barbero[4,5,6], Julie Bouckaert[3], Stipan Jonjic[1], Tihana Lenac Rovis[1*], Roberto Adamo[2*]

[1]Center for Proteomics, Faculty of Medicine, University of Rijeka, Rijeka, Croatia

[2]GSK Vaccines, Via Fiorentina 1, 53100 Siena, Italy

[3]Unité de Glycobiologie Structurale et Fonctionnelle, UMR 8576 du CNRS et Université de Lille, 50 Avenue de Halley, 59658 Villeneuve d'Ascq, France

[4]Chemical Glycobiology Lab CIC bioGUNE Technology Park, 48160 Derio, Spain

[5]Ikerbasque, Basque Foundation for Science, 48013 Bilbao, Bizkaia, Spain

[6]Department of Organic Chemistry II, University of the Basque Country, Universidad del País Vasco/Euskal Herriko Unibertsitatea, 48940 Leioa, Bizkaia, Spain

*** Correspondence:**
Corresponding Authors
tihana.lenac@uniri.hr; roberto.x.adamo@gsk.com

Keywords: Capsular polysaccharide, Neisseria meningitidis, Structural glycobiology, Glycoconjugates, Vaccines.

Abstract

Despite the considerable progress towards the eradication of meningococcal disease with the introduction of glycoconjugate vaccines, previously unremarkable serogroup X has emerged in recent years, recording several outbreaks through the African continent. Different serogroup X polysaccharide-based vaccines have been tested in pre-clinical trials, establishing the principles for further improvement. To elucidate the antigenic determinants of the MenX capsular polysaccharide, we generated a monoclonal antibody, and its bactericidal nature was confirmed using the rabbit serum bactericidal assay. The antibody was tested by inhibition enzyme-linked immunosorbent assay and surface plasmon resonance against a set of oligosaccharide fragments of different lengths. The epitope was shown to be contained within 5 to 6 repeating units. The molecular interactions between the protective monoclonal antibody and the MenX capsular polysaccharide fragment were further detailed at atomic level by saturation transfer difference NMR spectroscopy. The NMR results were used for validation of the in-silico docking analysis between the x-ray crystal structure of the antibody (Fab

fragment) and the modelled hexamer oligosaccharide. The antibody recognizes the MenX fragment by binding all 6 repeating units of the oligosaccharide via hydrogen bonding, salt bridges and hydrophobic interactions. In vivo studies demonstrated that conjugates containing 5-6 repeating units can produce high functional antibody levels. These results provide an insight on the molecular basis of MenX vaccine-induced protection and highlights the requirements for the epitope based vaccines design.

1 Introduction

Neisseria meningitidis (Men) is a gram-negative encapsulated diplococcus, capable of producing meningitis and sepsis in humans (1-3). Every year, thousands of cases and scores of deaths are recorded around the globe. However, the sub-Saharan African meningitis belt is by far the most affected area in the latest years (1, 4-8).

Most pathogenic Men are coated by a capsular polysaccharide (CPS) (9), as it improves colonization through evasion of the host's immune system (10). Based on the chemical composition of the CPS, Men is subclassified into twelve serogroups, being A, B, C, W, Y and X the most clinically relevant ones (4, 11, 12). Men CPS itself is highly immunogenic and elicits bactericidal antibodies in adult population (10), consequently, it has been widely used for the development of polysaccharide vaccines (3, 10, 12, 13). More recently, Men CPS has been covalently linked to immunogenic protein carriers, such as the chemically detofixied Diptheria or Tetanus Toxins (DT and TT, respectively) and the nontoxic mutant of diphtheria toxin, Cross-Reacting Material 197 (CRM_{197}), to form glycoconjugates (1). Men glycoconjugates based vaccines, such as Menactra, Menveo and Nimenrix (targeting MenA, C, Y, W) (1, 4, 11), have overcome most of the limitations of using plain Men CPS, i.e. lack of memory response, IgM-to-IgG maturation and ineffectiveness in children below 2 years of age (7, 11, 13-15). Over the last years, a MenA-TT conjugate, MenAfriVac, has been introduced in the so-called meningitis belt, leading to almost eradication of the disease (16).

MenX strains were first described in 1966 by Boris et al. (17, 18), yet, until recently, their association with invasive disease was not on pair with the other disease-causing serogroups (3). However, in the last years, several MenX outbreaks have been registered in the meningitis belt (6, 7, 12). The surge of MenX has alerted the World Health Organization (WHO), reclassifying this serogroup as a major threat (1). Particularly after the introduction of MenA mass immunization in Africa, serotype displacement of MenA carriage has been suggested as a contributing factor for the increase of MenX incidence (1). Alternatively (17), recent work from Ji et al showed that a MenX strain, isolated from a bacteremia case in China, derived from a MenA strain due to a capsule switching event (3).

Considering the potential emergence of MenX related meningococcal disease, (1, 3) it is indisputable that MenX disease possess a threat to global health, making the development of a vaccine a top priority (3).

Several MenX vaccines are already in preclinical trials, using MenX PS as vaccine antigen as the leading strategy (4). For example, a vaccine containing MenX CPS fragments conjugated to CRM_{197} has been successful at preclinical stage (1). A classic polysaccharide-protein conjugate approach is under investigation by the Indian Serum Institute for the development of a pentavalent *Men*ACXYW vaccine (NmCV-5). Other modern strategies include the vaccines containing enzymatic and chemically produced MenX oligosaccharides (OS) (2, 4).

The MenX CPS is composed by a repeating unit (RU) of N-acetylglucosamine-4-phosphate residues held together by α-(1-4) phosphodiester bonds (4). While this RU structure was first confirmed by ^{13}C NMR in 1974 (18, 19), little is known about the minimal antigenic determinant of the polysaccharide.

In vivo studies performed by Morelli et al. found that 3 RUs was the minimal antigenic portion of the CPS capable of eliciting protective antibodies (1). A synthetic fragment of 4 RUs has been also tested (11) in vitro, however these short lengths are considered suboptimal to elicit a robust immune response compared to the polysaccharide-conjugate. Therefore, despite dynamic simulation studies have hypothesized that 4RU could be the minimal epitope required for eliciting an immune response (14), it is general belief that longer fragments might be required to mimic the *in vivo* response achieved with conjugates of the native CPS (1, 5, 11). In this context enzyme based or combined chemo-enzymatic approaches have been used to develop conjugate vaccines based on oligomers of around 11 RUs which induced high levels of functional antibodies (2).

Despite these studies to investigate the potential of MenX polysaccharide in vaccine design, both structural antigenic determinant and minimal immunogenic epitope of MenX CPS have not been elucidated (11, 20). This minimal epitope is crucial to guide vaccine design particularly from synthetic approaches, where its length should ideally be short enough for practical synthesis while keeping representation of the native CPS conformation (14, 20, 21). Mapping interactions of glycans with protective antibodies epitopes is becoming a powerful tool to select glycans for epitope focused vaccines eliciting long lasting immunity and highly specific bactericidal antibodies (22). This principle has been successfully applied at preclinical level to generate glycoconjugate vaccines against *Clostrium difficile, S. pneumoniae*,Group B *Streptococcus*, and other bacteria (21, 23-25).

Herein, we isolated the first bactericidal monoclonal antibody against MenX polysaccharide and through an integrated approach based on ELISA, Surface Plasmon Resonance and STD-NMR we characterized its affinity towards the CPS and the positions involved in binding. The Fab was also crystallized to generate an in-silico model for the recognition with MenX CPS. The information generated from epitope mapping was utilized for the preparation of conjugates from different oligomer lengths. Combined data on the antigenic determinant involved in mAb recognition and on the minimal immunogenic portion support the notion that the minimal structural and immunogenic epitope of MenX CPS is comprised of 5-6 RUs.

2 Results

2.1 Selection and immunochemical characterization of a functional anti-MenX murine mAb

The anti-MenX CPS monoclonal antibody (mAb), clone MenX.01, was obtained using hybridoma technology. The glycoconjugate of *Neisseria meningitidis* serogroup X polysaccharide and CRM_{197} carrier protein (MenX-CRM_{197}) was used as immunogen (Figure 1a). Several attempts to immunize mice and obtain hybridoma cell lines were necessary to develop one monoclonal antibody that specifically recognizes MenX polysaccharide. In total, close to 6000 supernatants were tested for the binding assay on MenX polysaccharide (MenX-CPS) coated ELISA plates. Positive supernatants were re-tested and in parallel, a cross-reactivity test was performed on an irrelevant meningococcal glycoconjugate. This resulted in a single hybridoma cell line that secreted antibody specifically recognizing MenX-CPS, which was a kappa IgG1 isotype/subtype. Next, a large scale mAb production and purification was performed and the leading candidate, clone MenX.01, was purified from serum free medium by using one step affinity purification, in milligram scale. The purified MenX.01 mAb was tested against several structurally different polysaccharides to confirm the lack of cross-reactivity

between MenX CPS recognition and other bacterial carbohydrates (Figure 1b). The specificity of the MenX.01 mAb was further confirmed by immunostaining of MenX- CRM_{197} conjugate and CRM_{197} conjugated to Group B Streptococcus GBSII as control (Figure 1c), where the glycoconjugate MenX-CRM_{197}, showed its typical band on SDS PAGE. The bactericidal activity of the new mAb MenX.01 was then assessed through rabbit complement mediated serum bactericidal assay (rSBA). This assay is a surrogate of protection against Men disease (26) where it measures the vaccine-induced antibody potential to induce killing of Men in presence of rabbit complement (4). The bactericidal activity of the highly specific anti-MenX PS antibody, clone MenX.01, was tested in vitro. An rSBA titer of 1024 at 0.98 µg/mL demonstrated the recognition of live bacteria MenX strain Z9516 and the capacity of triggering complement-dependent cytotoxicity by MenX.01 mAb.

2.2 Conformational analysis of MenX capsular polysaccharide

MenX CPS is a homopolymer composed of α-(1-4)-phosphodiester linked N-Acetyl glucosamines (27). To understand if potential structural epitopes could be predicted, its conformational behavior and dynamic features were studied in silico using a combined theoretical (quantum mechanics -QM- and molecular dynamics -MD- calculations) and experimental (NMR) approach. Special attention was paid to the different torsion angles that define the glycosidic linkages and to the geometry of the six-membered rings.

First, to unravel the dynamic features at the glycosidic linkage of MenX capsular polysaccharide while reducing the cost of the computational study, we performed a long (1.0 µs) MD simulations of the simpler disaccharide (DP2) repeating unit, using the carbohydrate molecules specific GLYCAM06 force field, explicit solvent molecules and periodic boundary conditions as implemented in the Amber biomolecular simulation package (28). The results of the MD simulation indicated that in explicit water, the MenX DP2 assumes a typical *exo-syn* conformation around the ϕ torsion angle, which is strongly stabilized by the *exo*-anomeric effect. The Ψ torsion angle largely populates the *syn*-conformation ($\psi = -60°$), which is favoured by steric effects, although minor excursions to other regions of the conformational map such as the *syn+* and *anti* conformations (+60°, 180° degree respectively) are also possible. Instead, a higher degree of flexibility was observed for the α and β torsion angles. Specifically, the α angle shows a broad minimum around 0° degree ($-60° \leq \alpha \leq +20°$), while β is characterized by a larger flexibility, with low energy minima at 180°, -60° and 60° degrees (Figure 2A). Taken altogether, the results from the MD simulation shows that the energy profile for MenX DP2 explores different conformations, which differ for the combination of the flexible dihedral angles Ψ, α, and β, while keeping the ϕ torsion in the *exo*-anomeric conformation (Figure 2B).

The energy minima structures identified for the MenX DP2 disaccharide by the MD simulation were further evaluated using a QM approach at the B3LYP/6-31++g(d,p) level of theory, using the Gaussian 09 suite of programs (29) to derive their expected NMR parameters that were compared to those experimentally determined. In particular, the analysis of the scalar (J) coupling constants was used to define the conformational distribution around the glycosidic linkage. The comparison between the

experimental derived J-couplings and the calculated values confirmed the predominance of the *exo-syn* (ϕ = 60°) over the *exo-anti* (ϕ = -60°) conformation, which is probably present as minor conformation (Table S1, Supplemental Information). In agreement with the MD simulations previously described, the QM data also support the coexistence of different populations for the β torsion angle, while α is more restricted ($-50° \leq \alpha \leq 0°$) (Table S3, Supplemental Information).

Next, the identified structure of the DP2 disaccharide in its low energy conformation was used to build a longer dodecasaccharide fragment (DP12), as model of the entire polysaccharide. After submitting the DP12 to 1.0 μs MD simulation, results recapitulated those obtained for the simpler disaccharide with a few differences worth of mentioning. Briefly, the *exo-syn* conformation is preserved along the entire simulation. The ψ dihedral angle mainly populates the *syn*- (-60°) geometry, with minor excursions to the *syn*+ (+60°) and *anti* (±180°) regions. A similar behaviour for α and β dihedral angles is observed independently from the number of repeating units. Representative φ/ψ and α/β plots for DP12 are reported in Figure 2C. The analysis of the puckering of the six-membered rings showed that the low energy $^4C_1$ ring conformation is adopted by all residues along the entire simulation (data not shown). Overall, while a recent study has hypothesized that MenX CPS could display a large population of a helix-like geometry, especially for long polysaccharides, (14) the calculations performed herein for DP12 predict the existence of conformational flexibility mainly governed by the variability of β (mainly) and ψ, in a minor extent.

2.3 Selection of MenX CPS fragments for structural studies

The *in silico* analysis showed that MenX oligosaccharides display flexibility around the different torsional angles. Starting from this basic information provided by the calculations, the minimal MenX CPS portion able to recognize the functional MenX.01 mAb (30) was empirically determined. We produced oligomers of different lengths, i.e. average degree of polymerization (avDP) starting from the CPS. Mild acid hydrolysis and reaction monitoring by ^{31}P NMR spectroscopy allowed to obtain the fragments (Figure S1-2). From the final sample with avDP 11.7 we purified oligosaccharide (OS) fragments in the DP range from 1 to 11 (Figure 3a).

Competitive ELISA assay was carried out using different concentrations of the generated OS fragments (DP5.5–40 range) as inhibitors. MenX.01 mAb was incubated with increasing amounts of different OS fragments and later transferred to MenX CPS immobilized on ELISA plates (Figure 3b). Absence of primary antibody was used as negative control. Inhibition of mAb at shorter lengths was comparable between DP5.5, DP8 and DP10.5. The inhibition was increased by 0.5 log with DP15 and by 1 log with DP40 fragment, the later was slightly increased with the CPS. Therefore, competitive ELISA with the newly developed bactericidal MenX.01 mAb confirmed length-dependent recognition of the different fragments, that is, shorter fragments inhibited the interaction only at higher concentrations. The results also showed that avDP5.5 OS was sufficient to fully inhibit the binding of the mAb to the native CPS, thus containing the minimal epitope. This is in line with previous reports showing that 4

RUs were not sufficient to inhibit the binding of rabbit anti MenX specific serum, unless exposed as protein conjugate (11).

To measure the binding kinetics of MenX.01 mAb and to examine its binding to shorter DP fragments, additional studies were performed using Surface Plasmon Resonance (SPR). For this purpose, an avDP15 MenX conjugated to CRM_{197} was immobilized on a CM5 chip via the EDC chemistry (pH 5) at a level of 458 RUs. The interaction was fit through the 1:1 Langmuir binding model. The equilibrium constant K_d (µM) of 0.32 ± 0.04 x 10^{-6} fitted based on the kinetic constants $k_a = 8.64x10^3$ $M^{-1}.s^{-1}$, $k_d = 2.75x10^{-3}$ s, indicates a submicromolar affinity of the antibody for the MenX polysaccharide presented as a CRM_{197}-conjugate Figure 3c). The SPR kinetic analysis of the MenX.01 mAb showed that it binds with relatively fast on- and off-rates and moderate affinity to MenX, as typical for low affinity carbohydrate-protein interactions. In a competitive SPR study, we confirmed that DP5.5 retains an almost complete (75%) capacity to block MenX.01 binding, compared to CPS (Figure 3d). On the other hand, the minor fragment (DP2) had a very weak inhibitory capacity.

To gain further insights on the impact of carbohydrate length on binding, isothermal titration calorimetry (ITC) of OS in complex with the MenX0.1 mAb was performed. The obtained data indicated that the affinity for the MenX.01 mAb was very similar for DP5.5, 7 and DP9 (Table S3 and Figure S4, Supplemental Information), confirming that 5-6 RUs are sufficient to strongly bind to the mAb. The interactions of the antibody with MenX fragments appeared largely entropically driven, with only a small enthalpic contribution. The affinity (K_d) varied from ~2-3 µM for the smaller DP5.5-7, as measured by ITC, to ~0.3 µM, as determined for avDP15 by SPR (Table S3 Supplemental Information and Figure 3c, respectively).

2.4 Mapping of the MenX antigenic determinant by STD-NMR

Considering that above a length of 5-6 RU the capacity to bind to antibodies was similar to the CPS, the interaction of the DP7 and the mAb MenX.01 was investigated by STD-NMR to map positions involved in binding. The ^1H NMR spectrum is characterized by a distribution of the ring protons within a small range of chemical shifts, which renders possible to make only qualitative considerations. Following irradiation of the DP7-mAb complex at 7 or 8 ppm, it clearly appeared that all the protons from MenX repeating unit were receiving transfer of saturation (Figure 4), and particularly the positions H-1 and H-4 which are held together by the phosphodiester bridge connecting the proximal units. This indicates that the area surrounding these charged groups is likely involved in strong interactions with the binding pocket. Since the hydrogen atoms of the GlcNAc residues in the typical $^4C_1$ chair conformation point towards different spatial directions, the observed STD NMR response is the result of overall contribution of the different sugar units along the DP7 chain.

2.5 MenX.01 Fab X-Ray Crystallography

To determine the exact binding epitope of MenX.01 antibody on MenX sugar, we approached co-crystallization studies. For crystallization purposes, we produced different types of Fab fragments: Fab enzymatically obtained by digestion of MenX.01 IgG1 antibody with papain and recombinant Fabs, with and without His tag, by production in transiently transfected HEK293T cells. All the three Fab fragments were successfully purified and functional (the enzymatic Fab and the recombinant His Fab shown in Figure S3A-D), but none yielded crystals in co-crystallization studies. Then we produced a fourth Fab - IgG2a recFab-His. Functionality and an affinity close to that of the original MenX.01 antibody was demonstrated for this Fab (Figure S5, Supplemental Information). Co-crystallization studies of IgG2a recFab-His with the first smaller fragment of DP4 yielded crystals for X-ray analysis which diffracted at a resolution of 2.16 Å (Figure S6, Supplemental Information). Unfortunately, the crystals contained Fab alone and not of the Fab-DP4 complex. Attempts to soak the crystals with millimolar concentrations of DP5.5 and DP4 were without success. Therefore, the obtained crystal was used for docking studies as confirmation of the NMR data.

2.6 In Silico docking studies of MenX OS complexed with the mAb

To gain further insights into the molecular basis of recognition, the MenX hexasaccharide (DP6) was docked into the carbohydrate recognition domain (CRD) of the Fab region of the MenX.01 mAb. The DP6 structure, corresponding to the central section of the DP12 obtained by the MD simulations, was used as representative of the DP5.5 MenX minimal epitope (Figure 5). The CRD of the MenX.01 mAb shows an extended U-shaped groove running from the heavy to the light chains. Interestingly, most of the residues composing the CRD are positively charged amino acids (K5, R31, K75, K81, R97, R100 in the heavy chain, and K45, R55 in the light chain), which confer a high positive charge to the surface (Figure S7, Supplemental Information). Fittingly, the negatively charged phosphate groups of the MenX DP6 may, at least partially, satisfy the positively charged surface. Thus, the DP6 was docked into the CRD guided by the possible electrostatic intermolecular interactions among those groups. Next, a docking-minimization protocol of the complex was performed using the MAESTRO (Schrödinger) suite of programs (31). According to the calculations, the complex was conformationally stable and most of the intermolecular interactions were maintained, while new ones where found. In details, R31 and R100 establish electrostatic interactions with the phosphodiester groups at the termini of the oligosaccharide chain. Additionally, all six residues of the DP6 participate in hydrogen bond intermolecular interactions. In total, 9 hydrogen bonds within residues S33, N98, Y99, R100, G101, G26 and E50 stabilize the complex, with four of them mediated by the phosphodiester groups all along the carbohydrate chain (Figure 5). Finally, non-polar patches from the aromatic side chins of residues W52, Y99, Y32 and F27 also provide hydrophobic interactions to the DP6 oligosaccharide (Figure 5c). Interestingly, the phosphodiester groups at the edges of the DP6 oligosaccharide are instrumental to anchor the oligosaccharide chain to the mAb CRD through salt bridges with the R31 and R100 residues, at the termini of the CRD. Additionally, the internal sugar residues establish a variety of intermolecular interactions all along the extended groove. This

interaction pose is agreement with the STD NMR outcome, which suggested that DP6 is globally involved in mAb recognition.

2.7 Immunogenicity studies

In order to study the impact of the saccharide chain length on the sugar immunogenicity and assess whether the 6-mer identified as putative minimal epitope was able to elicit a robust and protective immune responses, the DP5.5, 10 and 20 fragments were conjugated to CRM_{197} to be tested in mouse animal model. Conjugation of MenX OS was achieved through a three-step procedure involving (i) reductive amination with a di-hydrazine linker to insert a hydrazine moiety and (ii) following reaction with di-N-hydroxysuccinimidyl adipate to transform the compound in a half ester for (iii) final coupling to the protein carrier. The obtained conjugates were characterized to determine the saccharide/protein ratio by protein and saccharide content determination, and the molecule profile by SDS-page and HPLC (Figure S8, Supplemental Information).

The prepared glycoconjugate vaccines were administered to mice at days 1, 14, 28 using a 1 µg/saccharide of each biomolecule. Sera sampling was collected 14 days after the second and the third dose. Sera were analyzed for anti-MenX PS IgG content by ELISA and for antibody functionality by SBA.

All the vaccines were able to induce a specific antibody response against the native MenX PS after the second dose that was boosted with the third dose (Figure 6). The DP5.5 was able to induce IgG levels comparable to the conjugated DP10, and with similar functional activity, clearly indicating that this sugar length represents the minimal epitope capable of inducing a strong immune response. The conjugated DP20 induced the best response from the set in terms of both antibodies and SBA titers, highlighting that further optimization of the immune response can be obtained by long fragments as result of the multiple exposition of the minimal epitope along the polysaccharide chain.

3 Discussion

In this study, we developed a highly specific antibody against MenX polysaccharide, clone MenX.01 which is showed to be bactericidal. Our structural and immunogenicity data converged establishing that MenX minimal epitope is contained within 5-6 RUs (DP5.5).

To our knowledge, currently there is only one monoclonal antibody, mAb 10B5F10, previously developed by Reyes et al. (32), that recognizes MenX CPS, whose bactericidal activity, however, was not assessed. Our bactericidal mAb is an IgG1 subtype, which could be connected to the dominance of this subclass production induced by alum adjuvanted vaccination with glycoconjugates (33, 34).

MenX.01 mAb was able to induce bactericidal killing at a concentration as low as 1 µg/mL (rSBA of 1024). An rSBA titer of ≥8 has been accepted as the correlate of protection for Men protective sera (35), however SBA protection threshold has not been defined for purified mAbs. Nevertheless, this protective mAb concentration seems realistic within the normal range of IgG in plasma, since other immunization studies in mice using pneumococcal conjugates have produced specific anti-PS IgG antibody concentrations in sera of ~10 µg/mL (36). Moreover, we found our rSBA titer similar to the anti-MenA PS mAb 7E1F7, which reported rSBA titers in the range of 0.49 to 0.122 µg/mL (37). Altogether, this is evidence that the produced mAb is bactericidal at physiological IgG concentration in sera.

In the case of homopolysaccharides, such as MenX CPS, identification of the conformation and orientation of the bound epitope to the corresponding antibody is challenging (38). Therefore, the first step was to have an estimate of the shortest OS which contained the minimal antigenic determinant for further characterization. In our competitive ELISA study, OS fragment avDP5.5 achieved full inhibition of the mAb-CPS binding. Furthermore, longer fragments, DP8 and DP10/11, did not increase the inhibition. This is an indication that the binding epitope is preserved above 5 RU. Shorter OS fragments, such as DP4, could be considered suboptimal epitopes. The higher inhibition observed with DP15 and larger fragments is most probably due to a multivalency effect. These longer fragments support multiple binding to their repeated epitopes, while no specific conformational structure could be predicted in silico for MenX CPS, SPR differences in the K_a/K_d values from mAb and Fab highlighted that an avDP5.5 was able to bind to the mAb similarly to the CPS.

Of the range of Fab fragments that we successfully produced and purified, only recombinant Fab-IgG2a-His yielded crystals. Co-crystallization with sugar fragments proved to be unsuccessful (38). In silico prediction on the MenX CPS conformation showed a high degree of flexibility in the polymer which prevents the formation of a preferential secondary structure, as opposed as a recent study highlighting potential formation of a helical structure for a length above 6 RU (14). Docking studies with a 6 RU fragment and the crystal structure of the Fab along with STD NMR analysis showed that indeed this length is sufficient to fully occupy the binding pocket. A network on hydrogen bonds involving the charged phosphate groups along with additional non polar patches would play a relevant role in stabilizing such interactions.

Finally, the identified epitope recognized by the functional mAb was conjugated to a carrier protein demonstrating to elicit an immune response similar to a longer avDP10. This clearly indicates that a length of 5-6 RU contains the minimal epitope of MenX CPS. The functional antibody levels were further increased for a conjugated avDP20 as result of multimeric presentation of the identified epitope.

In conclusion, our work identified a length of 5-6 RU as minimal structural and immunogenic epitope of MenX capsular polysaccharide. Further effort will be devoted to unravel fine details of the recognition of functional antibodies. This study highlights the importance of a structural approach for the rational selection of the polysaccharide fragments for vaccine development. In addition, this study can guide the design of minimal epitope based vaccines using synthetic or enzymatic methods.

4 Materials and Methods

4.1 Development of the anti-*Neisseria meningitidis* serogroup X polysaccharide (MenX-CPS) monoclonal antibody, clone MenX.01

The glycoconjugate of *Neisseria meningitidis* serogroup X polysaccharide with CRM_{197} carrier protein (MenX-CRM_{197}) (GSK, Siena, Italy) was used for BALB/c mice immunization (in groups of 3 mice). Immunogens were prepared by mixing MenX-CRM_{197} stock (2 µg polysaccharide content, diluted in phosphate buffer saline), with Alhydrogel® adjuvant 2% (aluminium content: 9-11 mg/ml) in 1: 9 alhydrogel: MenX-CRM_{197} ratio. The immunogen was prepared on the day of immunization and gently mixed at RT for 4-5 hours. Mice were subcutaneously immunized with MenX-CRM_{197} conjugate and Alhydrogel® adjuvant two times, at day 0 and 14. After second immunization, the sera of immunized BALB/c mice were screened for antibody titers against the MenX polysacharide (MenX CPS) (GSK, Siena, Italy) by using an enzyme-linked immunosorbent assay (ELISA) using plates coated with the respective polysaccharide. The mouse with the highest MenX titer was boosted one more time with the immunogen. Three days later, spleen cells were collected and, after lysis of red blood cells, fusion with SP2/0 myeloma cells at ratio 1:1 was performed. In total, 70 million lymphocyte cells were fused with 70 million fusion partner cells and plated on 6x 96-well plates. These hybridoma cell lines were cultured in 20% RPMI 1640 medium containing hypoxanthine, aminopterin, and thymidine for hybridoma selection. Cell growth was examined 2 weeks after fusion. In the first test, supernatants were screened by ELISA against MenX CPS and 18 positive hybridoma-motherwells were further propagated. The hybridoma-motherwells were retested next day and those with the retained positivity against MenX CPS (7 out of 18) were subsequently expanded and cloned by limiting dilution. Obtained cell lines were cultured and retested for their positivity against i) MenX-PS, ii) MenX-PS-CRM_{197} conjugate, iii) Protein carrier, CRM_{197} (GSK, Siena, Italy), iv) an irrelevant polysaccharide antigen, Group B streptococcus type II (GSK, Siena, Italy), and v) another irrelevant polysaccharide antigen, a meningococcal antigen, *Neisseria meningitidis* serogroup A polysaccharide (MenA-CPS) (GSK, Siena, Italy). Only one hybridoma-motherwell resulted in the antibody with the desired characteristics. Other attempts to obtain monoclonal antibodies against MenX CPS using 8 mice, with minimal variations in the immunzation protocol, did not yield additional antibody clones. Therefore, we generated one monoclonal antibody that specifically recognized MenX-PS and named it clone MenX.01. Large scale MenX.01 production was performed in RPMI 1640 media (PAN-Biotech GmbH) supplemented with FBS standard (PAN-Biotech GmbH) (10%), penicillin-streptomycin (PAN-Biotech GmbH) (final concentrations: penicillin 10 U/mL; streptomycin 10 µg/mL), L-Glutamine (PAN-Biotech GmbH) (final concentration: 0.2 mM) and β-Mercaptoethanol 50 mM in PBS (PAN-Biotech GmbH) (final concentration: 5 µM). The mAb was purified from the culture supernant, using GE AKTA Pure Liquid Chromatography System and HiTrap Protein G HP prepacked columns for preparative purification of monoclonal antibodies, in an amount of few milligrams.

4.2 Enzymatic Fab production

Affinity-purified MenX.01 mAb was concentrated to 2 mg/mL in PBS and cleaved into Fab and Fc fragments according to the protocol of Andrew & Titus (39). Briefly, purified antibody stock in PBS (2 mg/ml) was dissolved in freshly prepared 2x digestion buffer (0.035 M EDTA, 40 mM L-cysteine in PBS). Freshly prepared papain (0.1 mg/ml) was mixed in a 1:1 ratio with the antibody in 2x digestion buffer and incubated (37 °C, 2 hours). The reaction was stopped by the addition of iodoacetamide to a final concentration of 30 mM. The Fab fragment was purified from papain, Fc fragment and the undigested IgG on ÄKTA FPLC via tandem Protein G and Protein A affinity purification. Fab fragments were then concentrated in PBS centrifugal Amicon-filter concentrators (molecular weight separation 10 kDa) (Merck KGaA) to a final concentration of 1 mg/ml. The purity of the Fab was confirmed by SDS-PAGE analysis followed by SDS-PAGE and western blot/immunoblot analysis CPS (S Figure S3a-b).

4.3 Recombinant Fab production

The construction of the plasmids for recombinant Fab expressions were obtained by sequencing, synthesis and cloning by GenScript USA Inc. (New Jersey, USA). Briefly, from the selected hybridoma clone, RNA was reverse transcribed into cDNA. The antibody fragments of variable heavy chain (V_H) and variable light chain (V_L) were amplified, cloned into a standard cloning vector separately. Colony PCR was performed to screen for clones with inserts of the correct sizes and no less than five colonies with the correct insert size were sequenced. The resulting sequence is the consensus derived from the alignment of these clones (S, sequences).

The antibody fragment of V_H was synthesized and fused with either the IgG1 or the IgG2a first constant heavy chain domain (C_H1), the later was also designed to contain a 6x histidine tag at the C-terminal region. The V_L was processed similarly with the IgG constant kappa light chain domain (CL). The synthesized IgG1/IgG2a-kappa heavy and light chains were cloned separately into mammalian expression vector pcDNA3.4.

Transient expression of recombinant Fab was performed in either mono, tri or five-layer cell culture flask (Corning™ Falcon™ Fischer Scientific). HEK293T cells in RPMI 1640 media (PAN-Biotech GmbH) supplemented with FBS standard (PAN-Biotech GmbH) (10%), MEM NEAA (100x) (PAN-Biotech GmbH) and sodium pyruvate (PAN-Biotech GmbH) (final concentration 0.1 mM) were seeded 24 hours before transfection in order to achieve an 80% confluency next day. For each flask layer, the transfection mixture was prepared by mixing 19 µg of each heavy and light chain purified plasmids, 185 uL of polyethylenimine (PEI) solution (1 mg/mL) and 2.8 mL of DMEM media (PAN-Biotech GmbH) for 20-30 min at RT. Next, the flask media was removed, and the transfection mixture was added, after incubating for 2 minutes, the media was returned to the culture flask and the flask was placed back in the incubator. After 24 h, the media was exchanged with HyClone™ HyCell TransFx-H Medium (Cytiva, previously GE Healthcare) supplemented with MEM NEAA (100x) (PAN-Biotech GmbH), sodium pyruvate (PAN-Biotech GmbH) (final concentration: 0.1 mM), penicillin-streptomycin (PAN-Biotech GmbH) (final concentrations: penicillin 10 U/mL; streptomycin 10 µg/mL)and L-Glutamine (PAN-Biotech GmbH) (final concentration: 0.2 mM). Media was collected and replaced every 3-5 days for 1-2 weeks. The recombinant mouse Fabs were purified from the

supernatant using GE AKTA Pure Liquid Chromatography System equipped with a HisTrap HP columns packed with Ni Sepharose affinity resin. The Fab was analyzed by ELISA and western blot to confirm specific binding to MenX CPS (Figure S3c-d).

4.4 ELISA

Microtiter plates (96 wells, MICROLON® High Binding, Greiner Bio-One) were coated with polysaccharides (MenX-PS, MenA-PS, GBSII-PS), glycoconjugate MenX-CRM_{197} or CRM_{197} protein. 100 µL of CPS (5 µg/mL) in PBS pH 8.2 or 50 µL glycoconjugate/protein (2 µg/mL) in coating buffer pH 9.6 was added in each well. Plates were incubated overnight at 2-8 °C, washed two times with tap water and saturated with 150 µL/well PBST-B (3.0% Bovine Serum Albumin-BSA in PBST (0.05% Tween-20 in PBS pH 7.4)) for 1 hour at 37°C. The plates were flicked off to remove the solution and washed twice with tap water. The coated plates were incubated with mAb or Fab thereof in various dilutions, at room temperature for 1 hour, washed twice and incubated for 1 additional hour at room temperature with either anti-mouse IgG (H+L) Fc peroxidase (Jackson ImmunoResearch) diluted 1:1000 or anti-mouse IgG $F(ab')_2$ peroxidase (Jackson ImmunoResearch) 1:1000 diluted in PFT (1% FCS in PBST). After washing six times, the plates were developed with a 0.6 mg/mL solution of o-phenylenediamine dihydrochloride (OPD) (Sigma) in citrate buffer pH 5.5 and 0.001% of 30% hydrogen peroxide, at room temperature for 5-10 min. After stopping the reaction with 1M sulfuric acid, the absorbance was measured using a TriStar LB 941 multimode microplate reader with wavelength set at 490 nm and reference filter set at 630 nm. ELISA inhibition experiments were performed following the same procedure but pre-incubating the samples with one or more concentrations of the inhibitor for 20 min at room temperature.

4.5 Western blot/immunoblot analysis

CRM_{197} protein or MenX-CRM, MenA-CRM_{197} and GBSII-CRM_{197} glycoconjugates, in the amount of 2-10 µg, were separated by 8% SDS-PAGE electrophoresis. Fab fragments, in the amount of 2-10 µg, were separated on 10-12% SDS-PAGE electrophoresis. Samples were transferred onto 0.45 µm PVDF membrane (Hybond™, GE Healthcare) which were subsequently blocked with 5% w/v blotting grade low fat powdered milk (Carl Roth Gmbh & Co. Kg). Membranes were incubated with clone MenX.01 (mAb or Fab) overnight at 4°C. We used our own stock antibodies at a concentration of 1 mg/ml with a typical dilution of the primary antibody being 1:100. Protein signals were developed using anti-mouse IgG F(ab')2 peroxidase (Jackson ImmunoResearch) 1:1000 and visualized with an ImageQuant LAS 4000 mini camera system (GE Healthcare). Fab fragments were developed with either anti-mouse IgG F(ab')2 peroxidase (Jackson ImmunoResearch) diluted 1:1000 or anti-mouse IgG (H+L) Fc peroxidase (Jackson ImmunoResearch) diluted 1:1000 to confirm the absence of the Fc fragment in the preparation.

4.6 Complement-Mediated Bactericidal Activity (Rabbit Serum Bactericidal Activity Assay)

Serum bactericidal activity against *N. meningitidis* serogroup X strain Z9516 was evaluated as reported elsewhere (40), with minor modifications. Briefly, bacteria were grown overnight on chocolate agar plate (Biomerieux 43101) at 37°C in 5% CO_2. Colonies were inoculated in 7 ml of Mueller–Hinton

broth containing 0.25% glucose to an optical density at 600 nm (OD_{600}) of 0.05-0.06 and incubated at 37°C with shaking until early log phase [OD_{600} of ~0.25 corresponding to 10^9 colony-forming units per ml (CFU/ml)]. The cultured bacteria were diluted in Dulbecco's Phosphate Buffered Saline (DPBS-SIGMA D8662) containing 1% bovine serum albumin (BSA)(Sigma) and 0.1% glucose at the working dilution of 10^4-10^5 CFU/ml. The SBA was run in round bottom 96 well microplates in a final volume of 50 µl per well with 25 µL of serial two-fold dilutions of test sample (mAb and polyclonal Abs), 12.5 µL of bacteria at the working dilution, and 12.5 µL of active complement (25%). The bactericidal assay contains two internal controls: the first, to evaluate the bacterial killing by complement alone in the absence of antibodies, the second to evaluate the killing by serum alone in presence of heat inactivated complement. The reaction mixtures were incubated at 37°C for 60 minutes with 5% CO_2, then each sample was spotted on Mueller–Hinton agar plates. Serum bactericidal titers were defined as the mAb concentration resulting in 50% decrease in CFU/ml after a 60-min incubation of bacteria with the reaction mixture compared to the control CFU/ml at time zero.

4.7 Fragments of MenX polysaccharide preparation by mild hydrolysis

The DP40 OS depolymerization was performed by mild acid hydrolysis. A phosphodiester bond links *N. meningitidis* capsule building blocks, and the hydrolysis of this bond gives rise to a phosphomonoester bond. Therefore, measuring the ratio from the mono and diester bond is a way of following the hydrolysis reaction and estimate of the average degree of polymerization (DP) of the sample. The process was monitored by phosphorus (^{31}P) NMR spectroscopy, and it was quenched by neutralization when the desired average degree of polymerization (avDP) was reached. For a MenX OS target of avDP 5, the hydrolysis was performed in 50 mM NaOAc with saccharide concentration of 2.5 mg/mL at pH 4.0 and 80 °C, for ~18 h and two times overnight at RT. The reaction was quenched by neutralization with NaOH when ^{31}P NMR indicated an avDP of 11.7.

4.8 Purification of oligosaccharides

The fragments of different lengths were separated by anionic exchange chromatography using a semipreparative HPLC with a Sepharose Q column. By increasing the NaCl percentage of the elution buffer with a linear gradient, it was possible to isolate every oligosaccharide fragment in the range of 1-11 repeating units.

The length of the oligosaccharides was determined by ^{31}P NMR analysis. The ^{31}P NMR signals of phosphodiester in chain groups (P_{Int}) and phosphomonoester end groups (P_{Ter}) were integrated and used for avDP calculation:

$$\mathrm{avDP} = \left[\left(\frac{P_{Int}}{P_{Ter}}\right) + 1\right]$$

MenX OS's were desalted against water on a SEC Sephadex G-10 column (~0.3 mg of OS loaded per 1 mL of resin at 30 cm/h.

4.9 Surface Plasmon Resonance (SPR) analysis

Binding kinetics and affinities were determined by SPR using a BIACORE X100 system. Glycoconjugates of MenX were immobilized on research grade CM5 sensor chips (Biacore) using the amine coupling kit supplied by the manufacturer (Biacore). Immobilizations were conducted in 10 mM sodium acetate (pH 5) at sugar concentration of 30 µg/mL. The immobilized surface density was ~500 resonance units in each instance. Measurements were conducted in PBS Tween20 0.005% pH=7.2 at 25°C and at a flow rate of 45 µL/min. Following mAb or Fab binding, conjugate surfaces were regenerated with 3.5 M $MgCl_2$ and a contact time of 120 s. Sensorgram data were analyzed using BIAevaluation software (Biacore). For competitive SPR PBS Tween 0.005% pH=7.2 was used as the running buffer for the inhibition assays, at a 45 µl/min flow rate at 25°C. The experiment started with three start-up cycles to allow surface stabilisation. Each sample injection (120 s contact time, 300 s dissociation time) is followed by regeneration with 3.5 M MgCl2 (120 s contact time) to remove the bound analyte from the ligand immobilised on the chip surface. 10 µM MenX mAb MenX.01 has been used together with descending concentrations of MenX CPS, DP5, and DP2 (500 µg/mL, 250 µg/mL, 125 µg/ml, 62.5 µg/mL, 31.3 µg/mL, 15.6 µg/mL, 7.8 µg/mL, 3.9 µg/mL, 2 µg/mL, 1 µg/mL, 0.5 µg/mL, 0 µg/mL (no analyte in the mAb solution)).

4.10 Isothermal Titration Calorimetry (ITC) measurement

ITC experiments were performed with different concentrations of MenX.01 antibodies (~ 3, 6, 7 and 10 µM), at different temperatures (18°C, 25°C) and with different buffers (HEPES, PBS). The best results are obtained with 10.9 microM mAb and at 25°C in HEPES. For each of the MenX fragments DP7 and DP5.5, min 3 experiments were performed at different molar concentrations of the analyte.

4.11 STD NMR experiments

The interactions of the mAb MenX0.1 with DP7 in 1:50 molar ratio was studied by Saturation Transfer Difference (STD)-NMR using the pulse sequence from the Bruker library (stddiffesgp.3). Spectra were recorder at a 600 MHz at room temperature with 64 scans repeated in 64 loops in a matrix of 32k points in t2 in a spectral window of 6692.11 Hz centered at 2820.00 Hz. Excitation sculpting with gradients was employed to suppress the water proton signals. A spin lock filter (T1p) with a 2 kHz field and a length of 30 ms was applied to suppress protein background. Selective saturation of the protein resonances was performed by irradiating at 7.0 ppm (on resonance spectrum) using a series of shaped 90º pulses (50 ms, 1 ms delay between pulses) for a total saturation time of 2.0 s. For the reference spectrum (off resonance spectrum), the irradiation took place at 30 ppm. To obtain the 1D STD-NMR spectra the on-resonance spectra was subtracted from the off-resonance using Topspin 2.2 software. The difference spectrum corresponds to the STD-NMR spectrum and the intensity of its signals is proportional to the proximity of the corresponding protons to the protein. The STD was analysed using the amplification factor (A_{STD}). The amplification factor is obtained by multiplying the relative STD effect of a given proton (I_{STD}/I_0) at a given ligand concentration ($[L]_T$) with the molar ratio of ligand in excess relative to the protein ($[L]_T/[P]$), according to Equation

$$ASTD = \frac{I_0 - I_{SAT}}{I_0} X \frac{[L]_T}{[p]} = \frac{I_{STD}}{I_0} X \frac{[L]_T}{[p]}$$

Were A_{STD} is the STD amplification facto, I_0, I_{SAT} and I_{STD} are the intensities of the reference (off resonance spectra), saturated (on resonance spectra) and difference spectra, respectively. In order to get the epitope mapping information from the amplification factor, the relative A_{STD} with the highest intensity is set for 100%, and all the other signals are normalized accordingly.

4.12 Ab initio calculations

DFT calculations were carried out with the Gaussian 09 suite of programs. The geometry optimization and the scan analysis were performed utilizing Becke's hybrid three-parameter exchange functional and the nonlocal correlation functional B3LYP with the 6-31++g(d,p) basis set. Solvent effects were included using the polarizable continuum model (PCM) for water (IEF-PCM). Electronic energies were used to derive the energy profiles around the dihedral angles of interest (φ/ψ and α/β). Scalar coupling constants were computed for all the possible conformations (*exo*-*syn*, non-*exo* and *exo*-anti around φ, and gg, gt and tg around ω) using the GIAO method.

4.13 Molecular Dynamics Simulations

1 μs MD simulations of MenX DP2 and DP12 were performed using the AMBER12 and AMBER16 force fields within GLYCAM06 in explicit water. MenX DP2 and DP12 molecules were built using the GLYCAM carbohydrate builder web tool (http://glycam.org). The phosphate linkers were added using the xleap module of AMBER12 and the parameters and partial atomic charges were calculated with the antechamber module (derived from the DNA phosphodiester bond) using GAFF force field.

The resulting geometries were extensively minimized using conjugate gradients and then taken as starting structures for the MD simulations in explicit solvent.

The molecules were solvated in a theoretical box of explicit TIP3P waters and the solute atoms were positioned at least at 10 Å from the solvent box edge. The equilibration phase consisted on energy minimization of the solvent followed by an energy minimization of the entire system without restraints. The system was then heated up to 300 K during 100 ps followed by 2 ns dynamics at constant temperature of 300 K, controlled by the Langevin thermostat, and constant pressure of 1 atm. During the simulations, the SHAKE algorithm was turned on and applied to all hydrogen atoms (41). A cut-off of 8 Å for all non-bonded interactions was adopted. An integration time step of 2 fs was employed and periodic boundaries conditions were applied throughout. During the simulations, the particle mesh Ewald (PME) method was used to compute long-range electrostatic interactions (42-44). Minimization, equilibration, and production phases were carried out by the pmemd.cuda module of AMBER 12 and 16, while the analyses of the simulations were performed using cpptraj module from AMBERTOOLS 16 (45-47). Data processing and 2D plots were carried out using GNUplot softwares.

4.14 Docking studies

The MenX (DP6) hexasaccharide was built as already explained for DP2 and DP12. The global minimum conformer obtained from the analysis of DP2 and DP12 was taken as starting point for DP6 geometry. The molecule was then solvated in a theoretical box of explicit TIP3P waters, and the solute

atoms were positioned at least at 10 Å from the solvent box edge and counter ions were added to maintain electroneutrality. The equilibration phase consisted on, first, an energy minimization of the solvent followed by an energy minimization of the entire system without restraints, using the steepest descent algorithm. The resulting structure was placed into the CRD of the IgG2a antibody and manually docked to maximize the intermolecular interactions. The docked structures were then submitted to energy minimization with a low gradient convergence threshold (0.05) in 5000 steps. The OPLS_2005 force field was employed, as integrated in the MAESTRO (Schroedinger) suite of programs.

All figures were generated using the molecular graphic software PyMOL (The PyMOL Molecular Graphics System, Version 2.4 Schrödinger, LLC, http://www.pymol.org).

4.15 Protein crystallization

We set a series of crystallization conditions enzymatic or recombinant Fab with different OS lengths and determined the following optimal crystallization conditions. Crystals of recombinant Fab in complex with OS DP4 or DP5/6 were screened in a PACT premier™ (Molecular Dinamics) crystallization screen. Crystals were obtained in 0.2 M Potassium thiocyanate; 0.1 M Bis-Tris propane; pH6.5; 20% PEG 3350 Pact. Next, the crystals were soaked in cryosolvent 0,2 M Potassium thiocyanate; 0,1 M Bis-Tris propane; pH6,5; 27% PEG 3350 + 10% Glycerol and immediately quench cooled in liquid nitrogen prior to data collection.

X-ray diffraction data were collected at the SOLEIL Synchrotron (Soleil, France), on beamline PROXIMA 2A (PX2-A), and using a EIGER X 9M detector. Data were indexed and processed using XDS (48) and the CCP4 program suite (49). The structure of the complex was determined by molecular replacement in Phaser (50), using as template model coordinates from the structure of mouse Fab vFP05.01 (PDB code 5TKK). Refinement and manual model building were performed using Phenix (51) and COOT (52). Structure quality was assessed using (PDB entry code D7OO2). Figures were generated using PyMOL (http://www.pymol.org). Data collection and refinement statistics are reported in Table S4, Supplemental Information) (53).

4.16 *In vivo* studies

Protocols were approved by the Italian Ministry of Health (Approval number n. 804/2015-PR). All mice were housed under specific pathogen-free conditions at the GSK Vaccines Animal Resource Center in compliance with the relevant guidelines (Italian Legislative Decree n 26/2014). Three groups of eight female BALB/c mice were immunized by subcutaneous injection of glycoconjugates at 1 µg dose in saccharide content using alum phosphate as an adjuvant. Mice received the vaccines at days 1, 14 and 28. Sera were bled at days 0, 27 and 42.

Figures

Frontiers requires figures to be submitted individually, in the same order as they are referred to in the manuscript. Figures will then be automatically embedded at the bottom of the submitted manuscript. Kindly ensure that each table and figure is mentioned in the text and in numerical order. Figures must

be of sufficient resolution for publication (see here for examples and minimum requirements). Figures which are not according to the guidelines will cause substantial delay during the production process. Figure legends should be placed at the end of the manuscript. Please see here for full Figure guidelines

Conflict of Interest

MT, BB, DO, PH, MRR and RA are employees of GSK group of companies. MRR and RA are inventors of patents related to this topic. The remaining authors declare that the research was conducted in the absence of any commercial or financial relationships that could be construed as a potential conflict of interest.

Author Contributions

GP, JB, JJB, TLR, SJ and RA conceived the work; GP, MT, BB, DO, SR, PH, IC, VI, SM, KM, BL, SB, LU, EB, JR, MMR executed the work; GP, JB, TLR and RA wrote the manuscript; all contributed to the manuscript.

Funding

This work was sponsored by GlaxoSmithKline Biologicals and has received funding from the European Union's Horizon 2020 Research and Innovation Programme under the Marie Skłodowska-Curie Grant Agreement 675671 and from SJ ("Strengthening the capacity of CerVirVac for research in virus immunology and vaccinology", grant no. KK.01.1.1.01.0006, awarded to the Scientific Centre of Excellence for Virus Immunology and Vaccines and co-financed by the European Regional Development Fund).

Figure legends

Figure 1. Specificity and bactericidal functionality of the supernatants from the hybridoma cells producing mAb MenX.01 against MenX polysaccharide. A) MenX immunization protocol. B) Cross specificity test of purified MenX.01 mAb on ELISA plates coated with: i) MenX-PS, ii) i) MenA-PS, iii) GBSII-PS, iv) MenX-CRM_{197} conjugate and v) CRM_{197} protein. C) MenX-CRM_{197} molecules were detected by western blot/imunoblot using MenX.01 mAb followed by anti-mouse Fab-HRP. As a negative control, CRM_{197} and GBSII-CRM_{197} were used.

Figure 2. In silico conformational studies on MenX CPS. A) Glycosydic linkage analysis for DP2. The φ/ψ and α/β plots from 1 μs MD simulations in explicit water are shown (GLYCAM06 force field) for MenX DP2. The conformational flexibility at β is evident, while the other three torsion angles display more restricted motion. B) Structure of the global minimum for MenX DP2 as determined by MD calculations. C) Selected φ/ψ and α/β plots for different contiguous disaccharide fragments of MenX DP12 from the 1μs MD simulations in explicit water (GLYCAM06) carried out for the dodecasaccharide.

Figure 3. Identification of the MenX Antigenic Determinant by Competitive ELISA and SPR. A) Purification of different length MenX OS fragments. Sepharose Q column chromatography of depolymerized MenX CPS. B) MenX.01 inhibition ELISA using different length inhibitors. Different MenX fragments were used as inhibitors, MenX CPS and PFT buffer were used as positive and negative control, respectively. C) SPR Kinetic analysis of the MenX.01. binding kinetics and affinity constants of MenX.01 to MenX-CRM_{197} were determined by serial dilutions of the test antibody MenX.01. D) Comparison of MenX CPS, DP5.5 and DP2 relative capacity to block MenX.01 antibody binding by competitive SPR Study. Total capsular polysaccharide MenX DPS blocking was set at 100%.

Figure 4. STD NMR (D2O, 600 MHz) of a DP7 fragment in complex with MenX0.1 mAb. A) ^{1}H NMR of the oligosaccharide in the presence of MenX0.1 mAb (50:1 molar ratio). B) The STD NMR spectrum obtained for the complex upon on-resonance irradiation at 7 ppm; C) The STD NMR spectrum obtained for the complex upon on-resonance irradiation at 8 ppm. All sugar ring protons display transfer of saturation, with higher relative intensities for positions H-1 and H-4.

Figure 5. Docking of DP6 with MenX.01 Fab. A) Top and B) side view of the docking pose. The DP6 engages the mAb binding pocket from the heavy to the light chains in the CRD**.** C) Detailed intermolecular interactions in the docked-minimized structure of complex between MenX.01 Fab and MenX DP6 OS. The amino acids that contribute to the binding are indicated.

Figure 6. Immunogenicity of different length MenX OS conjugated to CRM_{197}. IgG and SBA titers measured after the second and third dose are reported. Data are obtained from immunization of eight female BALB/c mice by subcutaneous injection of glycoconjugates at 1 µg dose in saccharide content using alum phosphate as an adjuvant. Mice received the vaccines at days 1, 14 and 28. Sera were bled at days 0, 27 and 42. Dot represent single mice serum. Statistics was calculated with Mann-Withney.

References

1. Morelli L, Cancogni D, Tontini M, Nilo A, Filippini S, Costantino P, et al. Synthesis and immunological evaluation of protein conjugates of Neisseria meningitidis X capsular polysaccharide fragments. Beilstein J Org Chem. (2014) 10:2367-76.

2. Fiebig T, Romano MR, Oldrini D, Adamo R, Tontini M, Brogioni B, et al. An efficient cell free enzyme-based total synthesis of a meningococcal vaccine candidate. NPJ Vaccines. (2016) 1:16017.

3. Ji X, Yao PP, Zhang LY, Li Y, Xu F, Mei LL, et al. Capsule switching of Neisseria meningitidis sequence type 7 serogroup A to serogroup X. J Infect. (2017) 756:521-31.

4. Micoli F, Romano MR, Tontini M, Cappelletti E, Gavini M, Proietti D, et al. Development of a glycoconjugate vaccine to prevent meningitis in Africa caused by meningococcal serogroup X. Proc Natl Acad Sci U S A. (2013) 11047:19077-82.

5. Oldrini D, Fiebig T, Romano MR, Proietti D, Berger M, Tontini M, et al. Combined Chemical Synthesis and Tailored Enzymatic Elongation Provide Fully Synthetic and Conjugation-Ready Neisseria meningitidis Serogroup X Vaccine Antigens. ACS Chem Biol. (2018) 134:984-94.

6. Chen WH, Neuzil KM, Boyce CR, Pasetti MF, Reymann MK, Martellet L, et al. Safety and immunogenicity of a pentavalent meningococcal conjugate vaccine containing serogroups A, C, Y, W, and X in healthy adults: a phase 1, single-centre, double-blind, randomised, controlled study. Lancet Infect Dis. (2018) 1810:1088-96.

7. Muindi KM, McCarthy PC, Wang T, Vionnet J, Battistel M, Jankowska E, et al. Characterization of the meningococcal serogroup X capsule N-acetylglucosamine-1-phosphotransferase. Glycobiology. (2014) 242:139-49.

8. Lee D, Kim EJ, Kilgore PE, Takahashi H, Ohnishi M, Tomono J, et al. A Novel Loop-Mediated Isothermal Amplification Assay for Serogroup Identification of Neisseria meningitidis in Cerebrospinal Fluid. Front Microbiol. (2015) 6:1548.

9. Pizza M, Rappuoli R. Neisseria meningitidis: pathogenesis and immunity. Curr Opin Microbiol. (2015) 23:68-72.

10. Fiebig T, Berti F, Freiberger F, Pinto V, Claus H, Romano MR, et al. Functional expression of the capsule polymerase of Neisseria meningitidis serogroup X: a new perspective for vaccine development. Glycobiology. (2014) 242:150-8.

11. Harale KR, Dumare NB, Singh D, Misra AK, Chhikara MK. Synthesis of a tetrasaccharide and its glycoconjugate corresponding to the capsular polysaccharide of Neisseria meningitidis serogroup X and its immunochemical studies. Rsc Adv. (2015) 552:41332-40.

12. Ming SA, Cottman-Thomas E, Black NC, Chen Y, Veeramachineni V, Peterson DC, et al. Interaction of Neisseria meningitidis Group X N-acetylglucosamine-1-phosphotransferase with its donor substrate. Glycobiology. (2018) 282:100-7.

13. Fallarini S, Buzzi B, Giovarruscio S, Polito L, Brogioni G, Tontini M, et al. A Synthetic Disaccharide Analogue from Neisseria meningitidis A Capsular Polysaccharide Stimulates Immune Cell Responses and Induces Immunoglobulin G (IgG) Production in Mice When Protein-Conjugated. ACS Infect Dis. (2015) 110:487-96.

14. Hlozek J, Kuttel MM, Ravenscroft N. Conformations of Neisseria meningitidis serogroup A and X polysaccharides: The effects of chain length and O-acetylation. Carbohydr Res. (2018) 465:44-51.

15. Pecetta S, Tontini M, Faenzi E, Cioncada R, Proietti D, Seubert A, et al. Carrier priming effect of CRM197 is related to an enhanced B and T cell activation in meningococcal serogroup A conjugate vaccination. Immunological comparison between CRM197 and diphtheria toxoid. Vaccine. (2016) 3420:2334-41.

16. Trotter CL, Lingani C, Fernandez K, Cooper LV, Bita A, Tevi-Benissan C, et al. Impact of MenAfriVac in nine countries of the African meningitis belt, 2010-15: an analysis of surveillance data. Lancet Infect Dis. (2017) 178:867-72.

17. Tanir G, Ozsurekci Y, Lucidarme J, Yasar Durmus S, Lekshmi A, Akisoglu O, et al. Neisseria meningitidis Serogroup X ST-5799 (ST-22 complex) in Turkey: A unique pediatric case. Hum Vaccin Immunother. (2018) 141:209-12.

18. Garrido R, Puyada A, Fernandez A, Gonzalez M, Ramirez U, Cardoso F, et al. Quantitative proton nuclear magnetic resonance evaluation and total assignment of the capsular polysaccharide Neisseria meningitidis serogroup X. J Pharm Biomed Anal. (2012) 70:295-300.

19. Smith ICP. Determination of Composition, Sequence, and Conformation of Immunological Polysaccharides by C-13 Nuclear Magnetic-Resonance. T New York Acad Sci. (1974) 366:593-.

20. Carboni F, Angiolini F, Fabbrini M, Brogioni B, Corrado A, Berti F, et al. GBS type III oligosaccharides containing a minimal protective epitope can be turned into effective vaccines by multivalent presentation. J Infect Dis. (2019) 2216.

21. Oldrini D, Del Bino L, Arda A, Carboni F, Henriques P, Angiolini F, et al. Structure-Guided Design of a Group B Streptococcus Type III Synthetic Glycan-Conjugate Vaccine. Chemistry. (2020) 2631:6944.

22. Soliman C, Pier GB, Ramsland PA. Antibody recognition of bacterial surfaces and extracellular polysaccharides. Curr Opin Struct Biol. (2020) 62:48-55.

23. Broecker F, Hanske J, Martin CE, Baek JY, Wahlbrink A, Wojcik F, et al. Multivalent display of minimal Clostridium difficile glycan epitopes mimics antigenic properties of larger glycans. Nat Commun. (2016) 7.

24. Schumann B, Reppe K, Kaplonek P, Wahlbrink A, Anish C, Witzenrath M, et al. Development of an Efficacious, Semisynthetic Glycoconjugate Vaccine Candidate against Streptococcus pneumoniae Serotype 1. Acs Central Sci. (2018) 43:357-61.

25. Carboni F, Adamo R, Fabbrini M, De Ricco R, Cattaneo V, Brogioni B, et al. Structure of a protective epitope of group B Streptococcus type III capsular polysaccharide. P Natl Acad Sci USA. (2017) 11419:5017-22.

26. Acevedo R, Zayas C, Norheim G, Fernandez S, Cedre B, Aranguren Y, et al. Outer membrane vesicles extracted from Neisseria meningitidis serogroup X for prevention of meningococcal disease in Africa. Pharmacol Res. (2017) 121:194-201.

27. Bundle DR, Smith ICP, Jennings HJ. Determination of Structure and Conformation of Bacterial Polysaccharides by Carbon 13 Nuclear Magnetic-Resonance - Studies on Group-Specific Antigens of Neisseria-Meningitidis Serogroups a and X. J Biol Chem. (1974) 2497:2275-81.

28. Salomon-Ferrer R, Case DA, Walker RC. An overview of the Amber biomolecular simulation package. Wires Comput Mol Sci. (2013) 32:198-210.

29. M. J. Frisch GWT, H. B. Schlegel, G. E. Scuseria, M. A. Robb, J. R. Cheeseman, G. Scalmani, V. Barone, G. A. Petersson, H. Nakatsuji, X. Li, M. Caricato, A. Marenich, J. Bloino, B. G. Janesko, R. Gomperts, B. Mennucci, H. P. Hratchian, J. V. Ortiz, A. F. Izmaylov, J. L. Sonnenberg, D. Williams-Young, F. Ding, F. Lipparini, F. Egidi, J. Goings, B. Peng, A. Petrone, T. Henderson, D. Ranasinghe, V. G. Zakrzewski, J. Gao, N. Rega, G. Zheng, W. Liang, M. Hada, M. Ehara, K. Toyota, R. Fukuda, J. Hasegawa, M. Ishida, T. Nakajima, Y. Honda, O. Kitao, H. Nakai, T. Vreven, K. Throssell, J. A. Montgomery, Jr., J. E. Peralta, F. Ogliaro, M. Bearpark, J. J. Heyd, E. Brothers, K. N. Kudin, V. N. Staroverov, T. Keith, R. Kobayashi, J. Normand, K. Raghavachari, A. Rendell, J. C. Burant, S. S. Iyengar, J. Tomasi, M. Cossi, J. M. Millam, M. Klene, C. Adamo, R. Cammi, J. W. Ochterski, R. L. Martin, K. Morokuma, O. Farkas, J. B. Foresman, and D. J. Fox. Gaussian 09, Revision A.01. Gaussian, Inc, Wallingford CT; (2016).

30. Sharma N, Hanif S, Rana R, Upadhyay D, Chhikara MK. Evaluation of impact of temperature and pH alterations on the size and antigenicity of meningococcal serogroup A and X polysaccharides and conjugates. Vaccine. (2019) 377:965-72.

31. Schrödinger Release 2021-1: Maestro. New York, NY: Schrödinger, LLC; (2021).

32. Reyes F, Otero O, Camacho F, Amin N, Ramirez F, Valdes Y, et al. A novel monoclonal antibody to Neisseria meningitidis serogroup X capsular polysaccharide and its potential use in quantitation of meningococcal vaccines. Biologicals. (2014) 426:312-5.

33. Uddin S, Borrow R, Haeney MR, Moran A, Warrington R, Balmer P, et al. Total and serotype-specific pneumococcal antibody titres in children with normal and abnormal humoral immunity. Vaccine. (2006) 2427-28:5637-44.

34. Richter MY, Jakobsen H, Birgisdottir A, Haeuw JF, Power UF, Del Giudice G, et al. Immunization of female mice with glycoconjugates protects their offspring against encapsulated bacteria. Infect Immun. (2004) 721:187-95.

35. Findlow J, Balmer P, Borrow R. A review of complement sources used in serum bactericidal assays for evaluating immune responses to meningococcal ACWY conjugate vaccines. Hum Vaccin Immunother. (2019) 1510:2491-500.

36. Lee CJ, Lee LH, Frasch CE. Protective immunity of pneumococcal glycoconjugates. Crit Rev Microbiol. (2003) 294:333-49.

37. Madariaga S, Cedré B, García M, González E, Valerie Anne Ferro, R A. Evaluation of Bactericidal Activity of Monoclonal Antibodies Obtained from Neisseria meningitidis. Clinical Infectious Diseases: Open Access. (2018 (January 2019)) 2:3:2-5.

38. Haji-Ghassemi O, Blackler RJ, Martin Young N, Evans SV. Antibody recognition of carbohydrate epitopesdagger. Glycobiology. (2015) 259:920-52.

39. Andrew SM, Titus JA. Fragmentation of immunoglobulin G. Curr Protoc Cell Biol. (2003) Chapter 16:Unit 16 4.

40. Giuliani MM, Santini L, Brunelli B, Biolchi A, Arico B, Di Marcello F, et al. The region comprising amino acids 100 to 255 of Neisseria meningitidis lipoprotein GNA 1870 elicits bactericidal antibodies. Infect Immun. (2005) 732:1151-60.

41. Miyamoto S, Kollman PA. Settle - an Analytical Version of the Shake and Rattle Algorithm for Rigid Water Models. J Comput Chem. (1992) 138:952-62.

42. Darden T, York D, Pedersen L. Particle Mesh Ewald - an N.Log(N) Method for Ewald Sums in Large Systems. Journal of Chemical Physics. (1993) 9812:10089-92.

43. Essmann U, Perera L, Berkowitz ML, Darden T, Lee H, Pedersen LG. A Smooth Particle Mesh Ewald Method. Journal of Chemical Physics. (1995) 10319:8577-93.

44. Crowley MF, Darden TA, Cheatham TE, Deerfield DW. Adventures in improving the scaling and accuracy of a parallel molecular dynamics program. J Supercomput. (1997) 113:255-78.

45. Le Grand S, Gotz AW, Walker RC. SPFP: Speed without compromise-A mixed precision model for GPU accelerated molecular dynamics simulations. Comput Phys Commun. (2013) 1842:374-80.

46. Gotz AW, Williamson MJ, Xu D, Poole D, Le Grand S, Walker RC. Routine Microsecond Molecular Dynamics Simulations with AMBER on GPUs. 1. Generalized Born. J Chem Theory Comput. (2012) 85:1542-55.

795 47. Salomon-Ferrer R, Gotz AW, Poole D, Le Grand S, Walker RC. Routine Microsecond
796 Molecular Dynamics Simulations with AMBER on GPUs. 2. Explicit Solvent Particle Mesh Ewald. J
797 Chem Theory Comput. (2013) 99:3878-88.

798 48. Kabsch W. Xds. Acta Crystallogr D. (2010) 66:125-32.

799 49. Winn MD, Ballard CC, Cowtan KD, Dodson EJ, Emsley P, Evans PR, et al. Overview of the
800 CCP4 suite and current developments. Acta Crystallographica Section D-Structural Biology. (2011)
801 67:235-42.

802 50. Mccoy AJ, Grosse-Kunstleve RW, Adams PD, Winn MD, Storoni LC, Read RJ. Phaser
803 crystallographic software. J Appl Crystallogr. (2007) 40:658-74.

804 51. Liebschner D, Afonine PV, Baker ML, Bunkoczi G, Chen VB, Croll TI, et al.
805 Macromolecular structure determination using X-rays, neutrons and electrons: recent developments
806 in Phenix. Acta Crystallographica Section D-Structural Biology. (2019) 75:861-77.

807 52. Emsley P, Cowtan K. Coot: model-building tools for molecular graphics. Acta
808 Crystallographica Section D-Structural Biology. (2004) 60:2126-32.

809 53. Williams CJ, Headd JJ, Moriarty NW, Prisant MG, Videau LL, Deis LN, et al. MolProbity:
810 More and better reference data for improved all-atom structure validation. Protein Sci. (2018)
811 271:293-315.

812

Figure 1.TIF

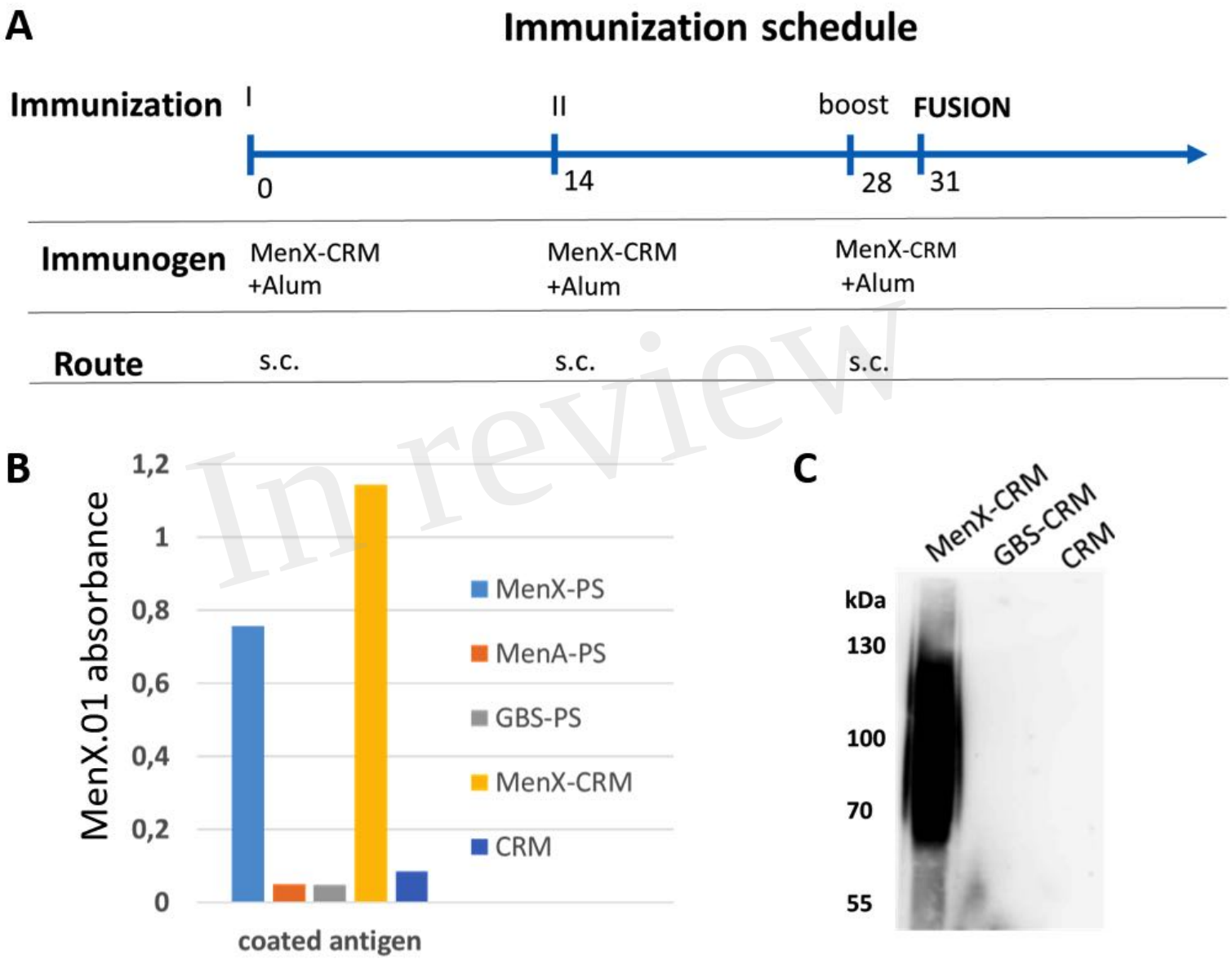

Figure 2.TIF

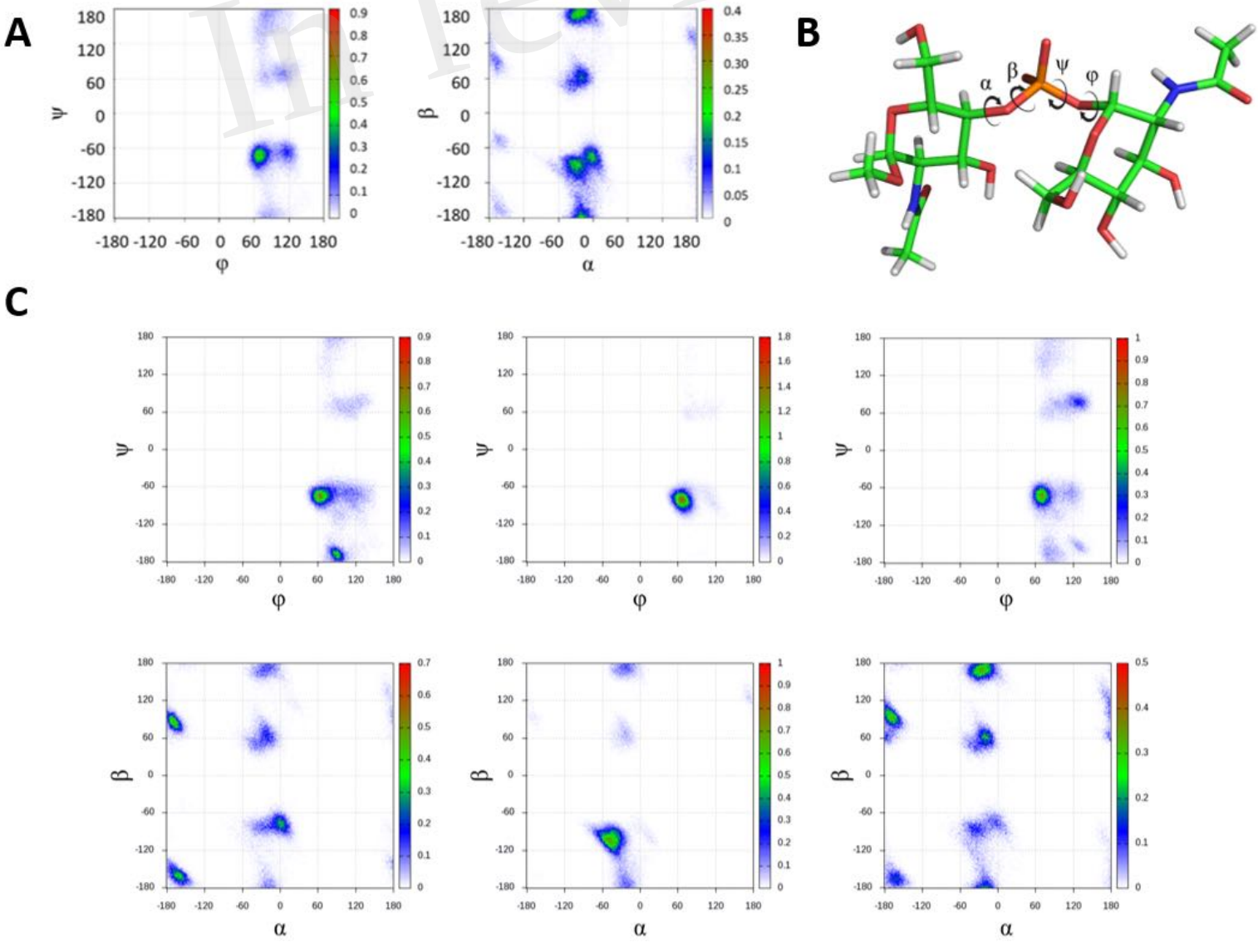

Figure 3.TIF

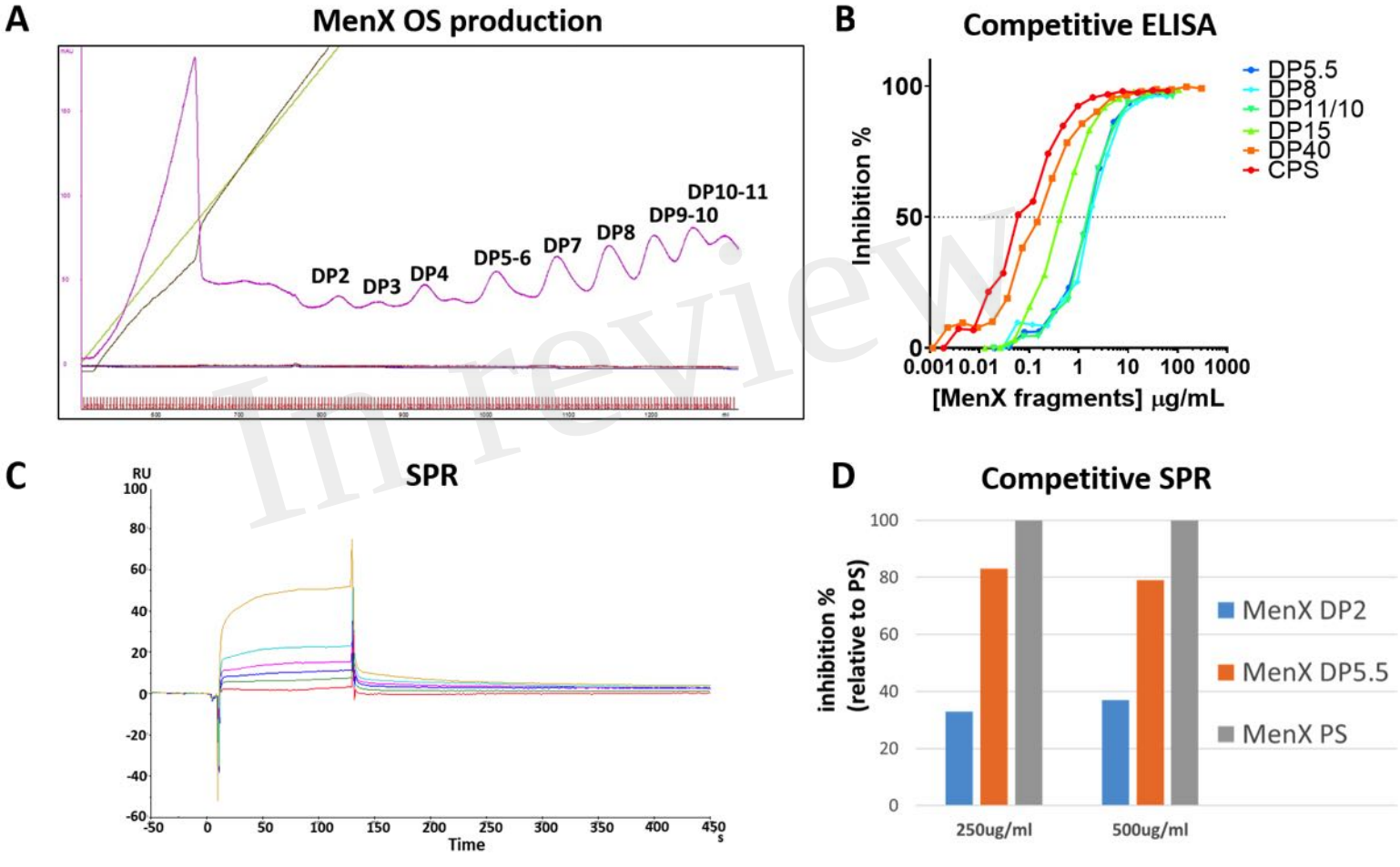

Figure 4.TIF

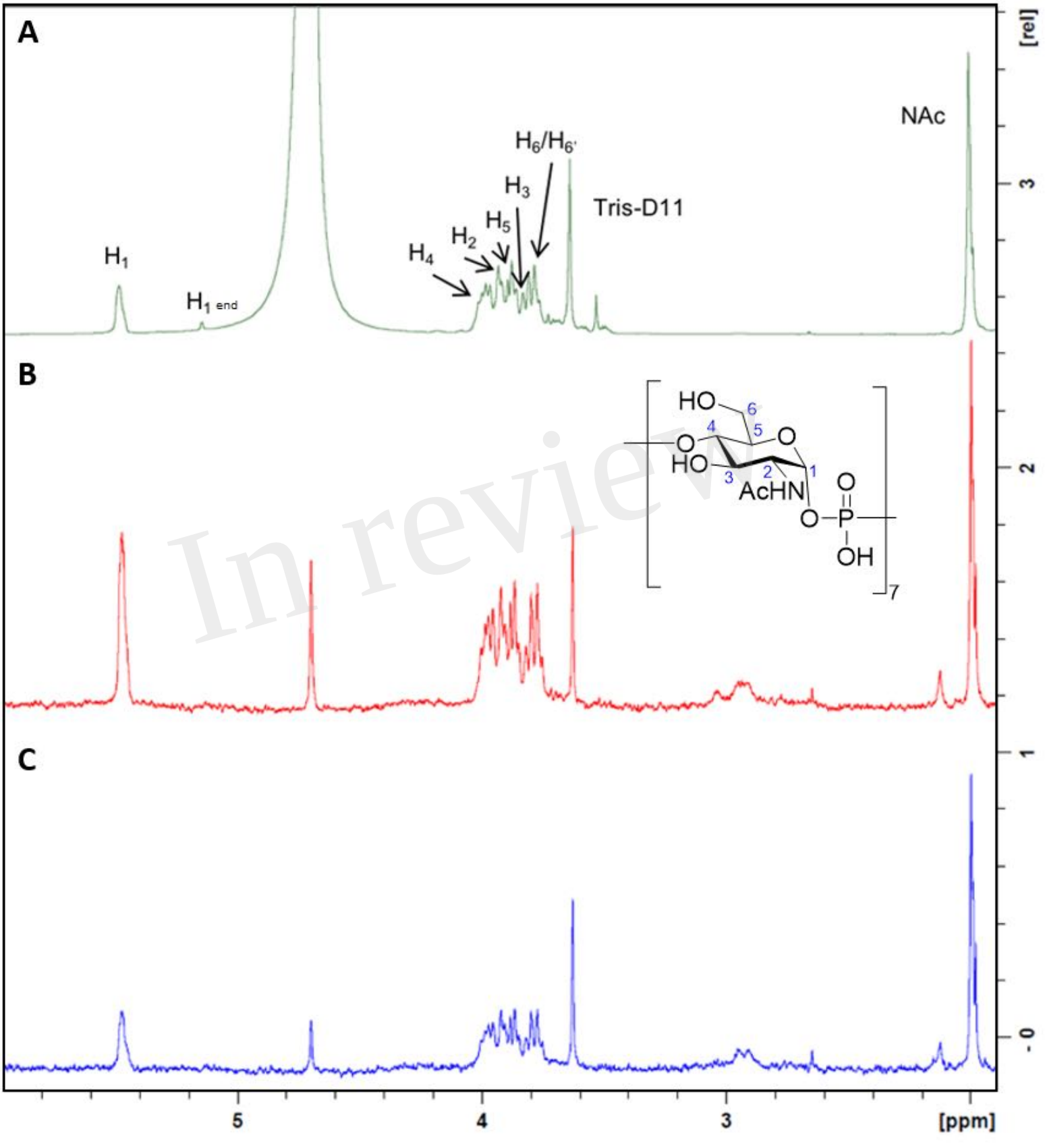

Figure 5.TIF

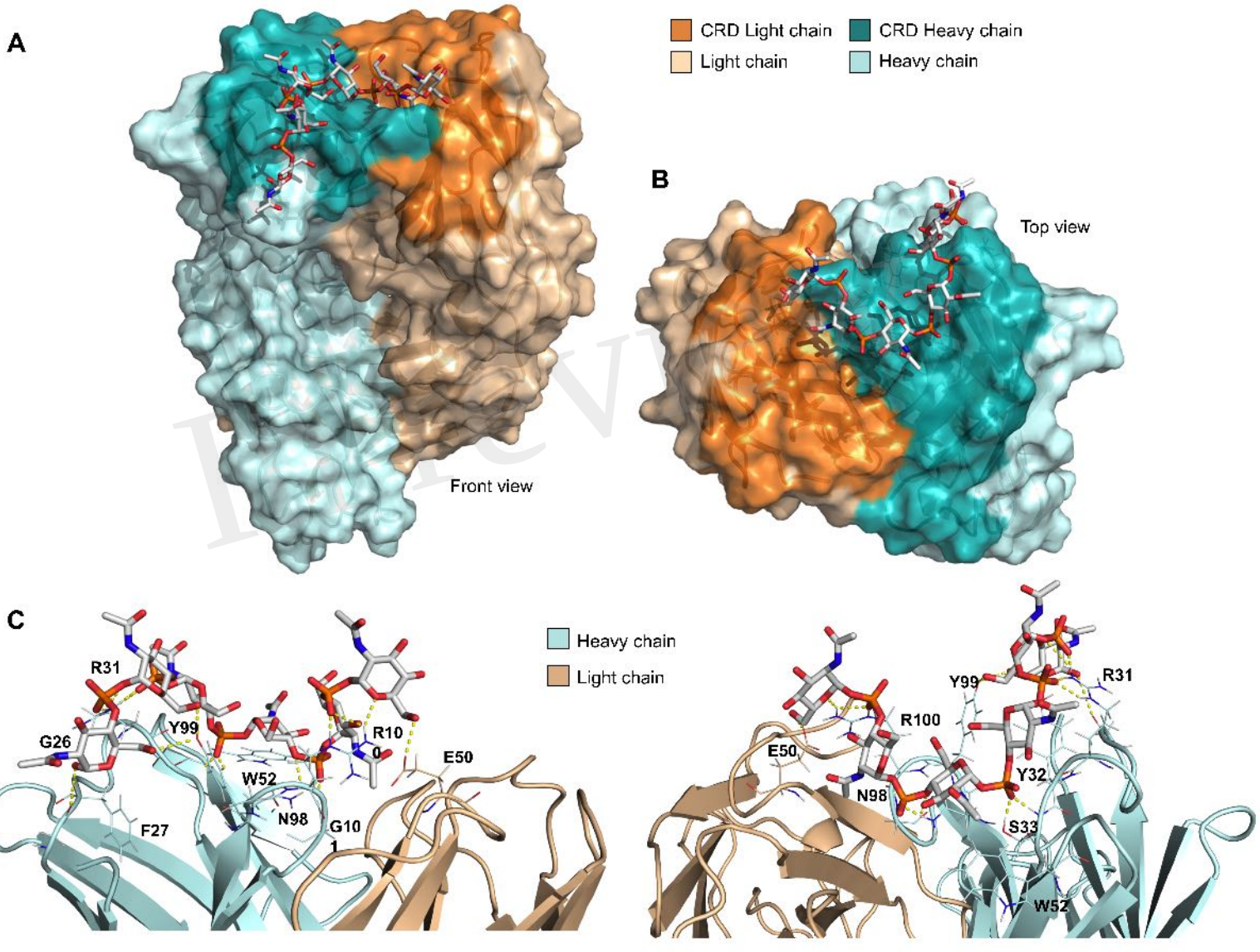
A
CRD Light chain
CRD Heavy chain
Light chain
Heavy chain
Front view
B
Top view
C
Heavy chain
Light chain
R31
G26
Y99
W52
F27
N98
G10
1
R10
0
E50
Y99
R31
R100
E50
N98
Y32
S33
W52

Figure 6.TIF

A

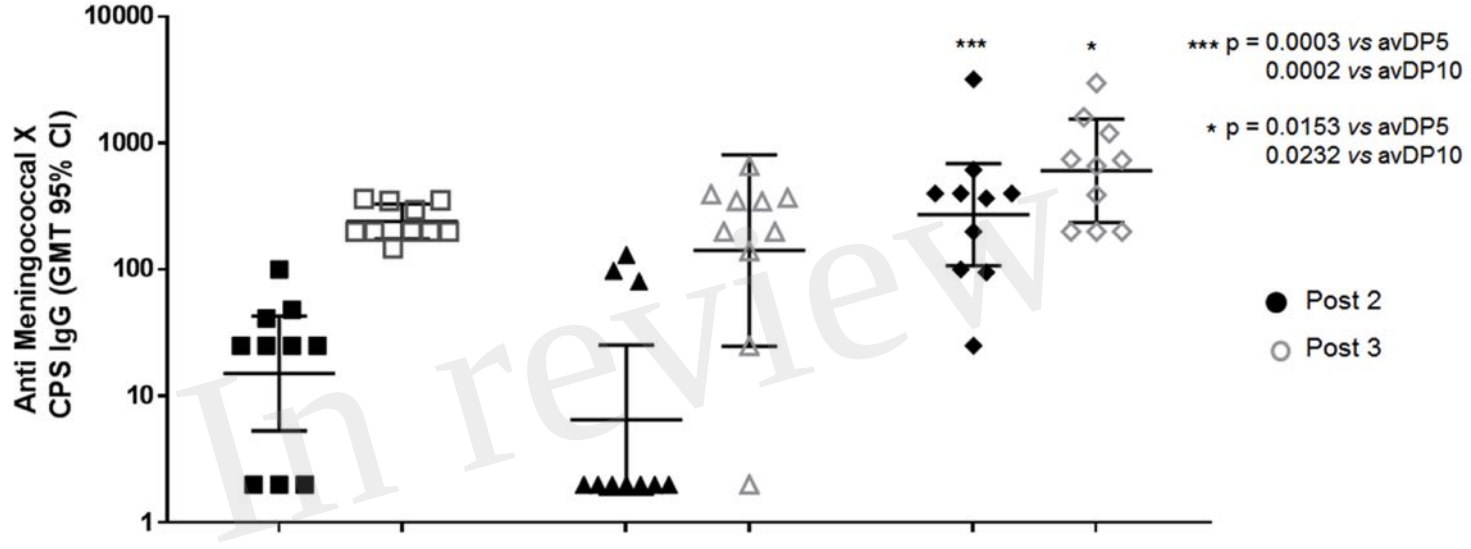

B

rSBA (MenX Z9516 strain)	**MenX-CRM$_{197}$ avDP5**	**MenX-CRM$_{197}$ avDP10**	**MenX-CRM$_{197}$ avDP20**
Post 2	64	32	1024
Post 3	1024	1024	8192